Measurement of Fe(α,α')Fe* Reactions Produced by 21-, 27.5-, and 47.9-MeV Alpha-Particle Bombardment: Statistical-Theory Analysis*

J. BENVENISTE
Aerospace Corporation, San Bernardino, California
AND
G. MERKEL†
Department of Chemistry, University of Rochester, Rochester, New York
AND
A. MITCHELL
Lawrence Radiation Laboratory, Livermore, California
(Received 26 July 1965)

The energy and angular distributions of inelastically scattered α particles from Fe have been measured at bombarding energies of 21, 27.5, and 47.9 MeV. The spectra are corrected for effects due to the presence of impurities in the target foil and to the energy degradation suffered as the α particles emerge from the target and pass through the forward portion of the detector. The energy and angular distributions have been analyzed with the semiclassical compound-nucleus theory of Ericson and Strutinski. In the analysis of the 21-MeV data, all of the inelastically scattered α particles are assumed to be emitted from the original compound nucleus. The angular distributions produced by the 27.5- and 47.9-MeV α-particle bombardment are found to be consistent with the nuclear moment of inertia determined from the 21-MeV data when multiple-particle-emission reactions such as Fe$(\alpha,n\alpha)$Fe or Fe$(\alpha,p\alpha)$Mn are included in the analysis. The inclusion of multiple-particle emissions in the statistical-theory analysis of the 27.5- and 47.9-MeV-induced reactions also significantly improves the agreement between experimental and theoretical energy distributions. In the statistical-theory analysis essentially two assumptions were made about the dependence of nuclear level density on nuclear spin and nuclear excitation energy. The first assumption was that the nuclear level density of a residual nucleus with spin J and excitation energy U is given by

$$\rho(U,J)=(\text{const})\,(2J+1)\,(U-\delta)^{-2}\exp\{2[a(U-\delta)]^{1/2}\}\exp(-\hbar^2J^2/2\mathcal{I}T),$$

where $T\cong(U/a)^{1/2}$ in the high-excitation-energy limit and $\mathcal{I}$ is the nuclear moment of inertia. The second assumption was that this equation is valid only when the excitation energy U is greater than approximately 6 MeV. For excitation energies below 6 MeV the nuclear density was assumed to be

$$\rho(U,J)=(\text{const})\,(2J+1)\exp[(U-\delta)/T_c]\exp(-\hbar^2J^2/2\mathcal{I}T_c),$$

where T_c, the nuclear temperature, is constant. The use of the second assumption involving a constant nuclear temperature in the excitation region below 6 MeV gave better over-all results than the use of the first assumption over the entire energy range. This second assumption is generally consistent with a nuclear phase transition, i.e., with the superconductor nuclear model.

I. INTRODUCTION

THE problem of interpreting nuclear reactions resulting in residual nuclei with excitation energies in the continuum is complicated by the presence of competing mechanisms. The two principal reaction mechanisms which may contribute to the observed cross sections are the direct reactions and the compound-nucleus reactions. Therefore, in studying the compound-nucleus reaction, one selects conditions which will enhance its contribution at the expense of the direct reaction.

Probably the most clear-cut feature distinguishing the two mechanisms is the reaction time. The direct reaction is fast (of the order of the time required to traverse the nucleus) while the compound-nucleus reaction is expected to be several orders of magnitude slower. Unfortunately, even these slow reaction times are shorter than 10^{-15} sec so that it is not now technologically possible to make a direct-time measurement the basis for the distinction.[1] Therefore, one is left with the study of other, less definitive features of the reaction products, such as excitation functions, energy distributions, and angular distributions.

The desirability of obtaining clear-cut evidence of compound-nucleus reactions has been increased by the theoretical work relating the angular distributions of reaction products to the statistical distribution of angular-momentum states in the excited nuclei. In the original development of the evaporation model[2–10] of

* The experimental portion of this work was performed when the authors were staff members of the University of California Lawrence Radiation Laboratory at Livermore.

† Present address: General Atomic Division of General Dynamics, John Jay Hopkins Laboratory for Pure and Applied Science, San Diego, California.

[1] T. Ericson, Advan. Phys. **9**, 425 (1960).
[2] N. Bohr, Nature **137**, 344 (1936).
[3] H. A. Bethe and R. F. Bacher, Rev. Mod. Phys. **8**, 82 (1936).
[4] V. F. Weisskopf, Phys. Rev. **52**, 295 (1937).
[5] V. F. Weisskopf and D. H. Ewing, Phys. Rev. **57**, 472, 935 (1940).
[6] L. Wolfenstein, Phys. Rev. **82**, 690 (1951).
[7] J. Blatt and V. F. Weisskopf, *Theoretical Nuclear Physics* (John Wiley & Sons, Inc., New York, 1952), p. 340.
[8] V. F. Weisskopf, in *Niels Bohr and the Development of Physics*, edited by W. Pauli (McGraw-Hill Book Company, New York, 1955), p. 134.
[9] A. M. Lane and R. G. Thomas, Rev. Mod. Phys. **30**, 257 (1958).
[10] G. R. Satchler, Oak Ridge National Laboratory Report No. ORNL-2606, p. 72 (unpublished).

the compound nucleus, it was assumed that the spin dependence of the nuclear level density was given by $\rho_J \propto 2J+1$. This leads to the prediction that the angular distribution of evaporation products is isotropic. There are theoretical reasons,[11–13] however, for believing that a more correct expression for the spin distribution is

$$\rho_J \propto (2J+1)\exp[-J(J+1)/2\sigma^2].$$

The spin cutoff parameter σ^2 is related to properties of the residual nucleus by the relation

$$\sigma^2 = \mathcal{I}T/\hbar^2,$$

where $\mathcal{I}$ is the nuclear moment of inertia and T, the nuclear temperature. Recently Ericson and Strutinski,[13] with a semiclassical approach, and Douglas and MacDonald,[14] with a quantum-mechanical treatment, have shown that, when the more correct spin-dependent level density is employed, the compound-nucleus theory yields anisotropic angular distributions which are symmetric about 90 deg, and that the parameter σ^2 is related to the magnitude of the anisotropy. The methods of statistical mechanics have long been applied to nuclear models for the calculation of nuclear level densities. The most widely used nuclear model has been that in which the nucleons behave as independent particles.[11–13,15,16] A number of authors have examined the effect of nuclear shell structure on the value of σ^2 and on nuclear level densities in general.[17–24] Bethe[11,12] viewed the nucleus as an infinite square well containing a Fermi gas and obtained a nuclear moment of inertia corresponding to that of a rigid rotor, i.e., $\mathcal{I}=\frac{2}{5}MR^2$, where M is the nuclear mass and R the nuclear radius. Bloch[18] used a harmonic oscillator potential and obtained $\mathcal{I}=\frac{1}{4}MR^2$. More recently, a number of authors have included the effect of nucleon pairing correlations on the parameter σ^2 and on nuclear level densities in general.[18,25–32]

This report describes attempts to evaluate the important parameter σ^2 over a wide range of excitation energies by measurements of the energy distribution and angular distribution of α particles inelastically scattered from Fe. A medium-weight element was selected so that the level densities of the compound and residual nuclei would be sufficiently high that the statistical assumption would be valid; while at the same time, the Coulomb barrier be not so high as to preclude the emission of the low-energy particles which make up such a large fraction of the compound-nucleus cross section.

The largest compound-nucleus α-particle emission probabilities from nuclei in the mass region of Fe occur for α particles emitted with an energy of approximately 10 MeV. For α particles emitted with energies above this, the lack of complete symmetry about 90 deg indicates a significant direct-interaction component. In the past, (α,α') experiments, in which an attempt was made to obtain compound-nucleus data, were hampered by experimental techniques which limited the minimum observed α-particle emission energy.[33–36] In the experiments described here every attempt was made to measure, accurately, inelastically scattered low-energy α particles by employing thin target foils and a dE/dx counter which was as thin as is consistent with accurate particle-naming with the dE/dx-E method.

We have attempted to obtain compound-nucleus data for a large range of residual nucleus exictation energies by varying the incident α-particle energy and observing inelastically scattered α particles with energies in the region of 10 MeV. A complication that arises in this approach is the emission of particles in cascade. When the incident α-particle energy is high enough, the observed inelastically scattered α particle need not necessarily be from the original compound nucleus which was produced by the bombarding particle plus the target nucleus. The possibility of α-particle emission after the emission of a neutron, proton, etc., must be considered in the analysis of the experimental results.

The statistical theory predicts absolute cross sections, angular distributions, energy distributions, and the variation of these measurable properties as a function of incident-projectile energy.[7] In this paper we attempt, in a limited and simplified manner, to compare the predictions of the statistical theory with all of these experimentally measurable properties. Unfortunately, a completely rigorous statistical-theory treatment, while possible, is extremely unwieldy.

An important question yet to be answered in a sufficiently quantitative manner is whether or not statistical randomness is achieved in compound-nucleus reactions involving excitation energies as high as 50 MeV. It is

[11] H. A. Bethe, Phys. Rev. **50**, 332 (1936).
[12] H. A. Bethe, Rev. Mod. Phys. **9**, 69 (1937).
[13] T. Ericson and V. Strutinski, Nucl. Phys. **8**, 284 (1948).
[14] A. C. Douglas and N. MacDonald, Nucl. Phys. **13**, 382 (1959).
[15] C. van Lier and G. E. Uhlenbeck, Physica **4**, 531 (1937).
[16] J. Bardeen, Phys. Rev. **51**, 799 (1937).
[17] H. Margenau, Phys. Rev. **59**, 627 (1941).
[18] C. Bloch, Phys. Rev. **93**, 1094 (1954).
[19] T. D. Newton, Can. J. Phys. **34**, 804 (1956).
[20] N. Rosenzweig, Phys. Rev. **105**, 95 (1957).
[21] N. Rosenzweig, Phys. Rev. **108**, 817 (1957).
[22] A. A. Ross, Phys. Rev. **108**, 720 (1957).
[23] A. G. W. Cameron, Can. J. Phys. **36**, 1040 (1958).
[24] T. Ericson, Nucl. Phys. **8**, 265 (1958).
[25] T. Ericson, Nucl. Phys. **6**, 62 (1958).
[26] V. Strutinski, in *Comptes Rendus du Congrès International de Physique Nucléaire; Interactions Nucléaire aux Basses Energies et Structure des Noyaux, Paris, July, 1958* (Dunod Cie, Paris, 1959), p. 617.
[27] J. M. B. Lang and K. J. LeCouteur, Proc. Phys. Soc. (London) **A67**, 586 (1959).
[28] K. J. LeCouteur and D. W. Lang, Nucl. Phys. **13**, 32 (1959).
[29] D. W. Lang and K. J. LeCouteur, Nucl. Phys. **14**, 21 (1959/60).
[30] D. W. Lang, Nucl. Phys. **42**, 353 (1963).
[31] M. Sano and S. Yamasaki, Progr. Theoret. Phys. (Kyoto) **29**, 397 (1963).
[32] P. Brovetto and V. Canuto, Nucl. Phys. **44**, 151 (1963).
[33] G. Igo, Phys. Rev. **106**, 256 (1957).
[34] H. W. Fulbright, M. O. Lassen, and N. O. Roy Poulsen, Kgl. Danske Videnskab. Selskab, Mat. Fys. Medd. **31**, No. 10 (1959).
[35] G. Merkel, University of California Radiation Laboratory Report No. UCRL 9898, 1961 (unpublished).
[36] C. R. Gruhn and L. W. Swenson, Bull. Am. Phys. Soc. **8**, 357 (1963).

hoped that the work to be described here will contribute to the resolution of this question.

II. DESCRIPTION OF EXPERIMENT

These experiments, at 21 and 27.5 MeV, were performed at the Livermore variable-energy cyclotron, and at 47.9 MeV, at the Crocker Laboratory cyclotron on the University of California campus at Berkeley. For the most part, the techniques used were the same.[37]

The α beam was magnetically analyzed, focused, and then collimated to a diameter of $\frac{1}{8}$ in. prior to entering the scattering chamber. A remotely rotatable table in the scattering chamber has provision for quickly and accurately mounting a detector on it. At the center of the chamber is a remotely controlled target changer. The target changer is geared so that it rotates at half the rate of the detector angle; thus, the target normal always bisects the scattering angle. (At the Crocker installation, the target-angle readout was considered unreliable so the scatterer was immobilized at an angle of 45 deg to the beam direction.) After traversing the scattering chamber, the beam was collected in a Faraday cup. A biased grid just ahead of the cup suppressed the loss of secondary electrons from the Faraday cup. (At Crocker the same function was performed by means of a magnet.)

The bombarding energy is measured by scattering a portion of the incident beam 90 deg through a variable absorber into a double proportional counter. An anticoincidence arrangement permits a differential range measurement of the scattered particles. A correction for absorption in the scatterer is made prior to the application of the range-energy relations. A final correction for the energy lost to the recoiling nucleus yields the bombarding energy.

Back of the proportional counters is a CsI crystal and photomultiplier tube. After the range has been measured, enough absorber is left in to allow only a small fraction of the incident energy to be deposited in the crystal. Pulses from the photomultiplier are fed into a "continuous energy monitor," a device which measures the average height of input pulses and yields a continuously visible meter reading. Sensitivity checks show that in the course of a run the bombarding energy is kept constant within $\pm 0.1\%$.

At the Crocker 60-in. cyclotron, the beam was steady enough to measure the range of incident particles by noting the current collected by the Faraday cup as a function of thickness of aluminum absorber interposed. The half-current thickness was taken as the range. Since this is a fixed frequency cyclotron, there was very little problem with beam energy variations, and no attempt was made to monitor them continuously.

The scatterer is an unbacked foil of natural Fe, 1.5 mg/cm^2 thick. It was produced by Wm. Brunner of the Livermore Laboratory, using a vacuum-evaporation and deposition technique.

The detector is a silicon p-n junction diode preceded by a gas proportional counter with offset center wire. Together with a pulse multiplier network, this assembly constitutes a "particle namer" in that the multiplied output is a pulse whose size is characteristic of the type of particle detected. This pulse is used to gate the multichannel analyzer to ensure that only the spectrum of α particles seen by the solid-state detector is recorded. It should be mentioned that with the settings used it is not possible to distinguish He^3 nuclei from α particles. However, it is assumed that the contribution of the former is small enough to ignore.

The response of the detection system (silicon p-n junction to pulse-height analyzer) was measured in a series of calibration runs. A Mylar target (≈ 1 mg/cm^2) was inserted in the beam and the spectrum of scattered α particles was observed at several angles. The energies of scattered particles leading to the well-known final states of C^{12}, O^{16}, and H^1 were calculated from the kinematics of the reaction. These were plotted versus the pulse-height response of the solid-state detector to yield the calibration curve of Fig. 1. The departure from linearity is due to self-absorption in the foil and the energy loss suffered by the particle as it traverses the proportional counter. When the proper correction is made for this energy loss, the calibration curve becomes straight and it passes through the origin.

III. ANALYSIS OF DATA

The major impurities found in the Fe target were carbon and oxygen. These were detected by observation of characteristic peaks superimposed on the evaporation spectra of Fe, Fig. 2(a). If it were just these peaks that appeared, the impurity correction would have been trivial since peaks are easy to identify and subtract. However, it was the contribution of the im-

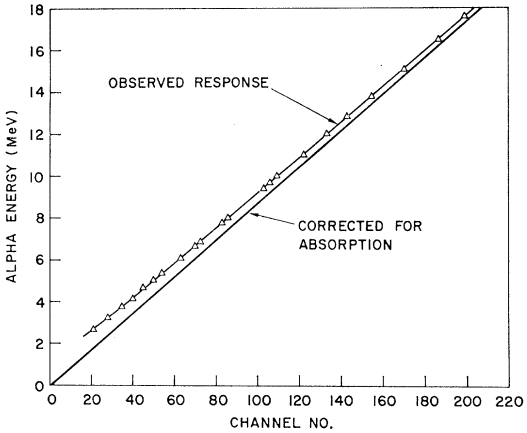

FIG. 1. Calibration curve of solid-state detector response (Mylar points).

[37] J. Benveniste, R. Booth, and A. Mitchell, University of California Radiation Laboratory Report No. UCRL 7427, 1963 (unpublished).

purities to the continua which gave the most trouble. This is because both C^{12} and O^{16} may break up into several α particles following inelastic scattering[38] to highly excited states, and because the relatively low Coulomb barrier permits a large fraction of the low-energy α particles to emerge. This meant that below about 6 MeV the major fraction of the α particles observed came from impurities which constituted about 1% of the target nuclei.

To make a proper impurity correction, scattered α-particle spectra from C^{12} and O^{16} were obtained at each bombarding energy for scattering angles up to 90 deg. Beyond this the continuum was not observed because of center-of-mass motion. Separate C^{12} and O^{16} spectra were obtained by first bombarding a polyethylene $[(CH_2)_n]$ foil to give the C^{12} spectrum, then bombarding a Mylar $[(C_{10}H_8O_4)_n]$ foil and subtracting a C^{12} spectrum whose characteristic peaks had been normalized to yield the O^{16} spectrum. Impurity corrections were made at each angle ($\leq$90 deg) by normalizing the individual C^{12} and O^{16} spectra to the characteristic peaks which appeared on the Fe spectra. The largest corrections occurred at 30 deg. Referring to Fig. 2(b), they amounted to 30% at an exit-channel energy of 6.5 MeV and decreased rapidly above that. Figure 2(c) shows data for which no impurity correction was necessary.

The shape of the spectrum of detected α particles is distorted by the effect of absorption in the scatterer and in the proportional counter ahead of the solid-state detector. To correct for this effect, it is assumed[37] that we may write for the rate of energy loss of α particles

$$dE/dx=-k/E^n,$$

where k and n are constants which are chosen to fit the data in the region of interest ($6<E_\alpha<15$ MeV). Then

$$-\int_{E_R}^{0} E^n dE=k\int_0^R dx$$

$$R=[k(1+n)]^{-1}E_R^{n+1},$$

where E_R denotes the real energy of the observed α particle, and

$$R-(\Delta x+\tfrac{1}{2}t)=[k(n+1)]^{-1}E_0^{n+1},$$

where Δx and $\frac{1}{2}t$ are the aluminum equivalents of the proportional counter and half the scattering foil thickness, respectively, and E_0 is the observed energy of the α particle. Thus,

$$E_R^{n+1}=E_0^{n+1}+(n+1)k(\Delta x+\tfrac{1}{2}t)$$

or converting to channel numbers

$$N_R^{n+1}=N_0^{n+1}+\frac{(n+1)k}{(e/c)^{n+1}}(\Delta x+\tfrac{1}{2}t),$$

where e/c (energy/channel) is the slope of the corrected calibration curve of Fig. 1.

This expression gives us the proper channel number in

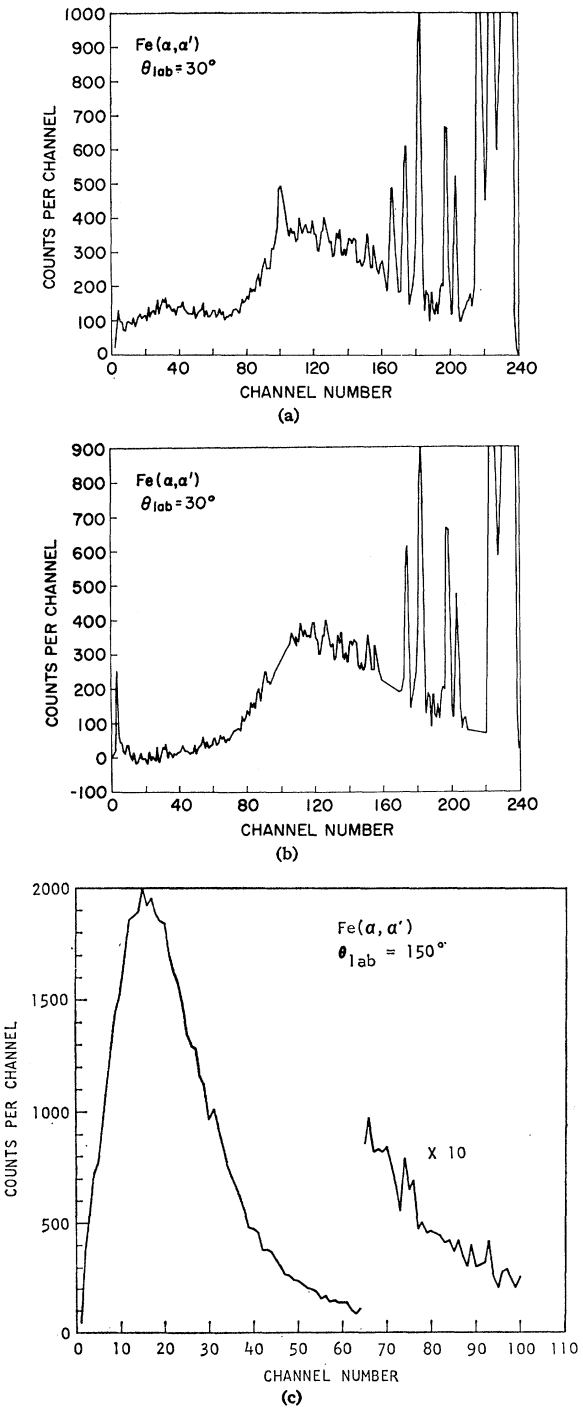

FIG. 2. (a) Typical 21-MeV Fe spectrum before subtraction of impurity contributions; (b) typical 21-MeV Fe spectrum after subtraction of impurity contributions; (c) typical 47.9-MeV Fe spectrum. No impurity correction was necessary for laboratory angles greater than 90 deg.

[38] L. B. Brown and H. B. Knowles, Phys. Rev. **125**, 1339 (1962).

terms of the observed channel number; however, a further correction is necessary for the spectral shape—the actual number of counts per channel in terms of the observed counts per channel.

The relation between the actual and observed spectra is

$$S_R(N_R)dN_R=S_0(N_0)dN_0.$$

Since

$$dN_0=(N_R/N_0)^n dN_R,$$

$$S_R(N_R)=S_0(N_0)\left[1+\frac{(n+1)k(\Delta x+\frac{1}{2}t)}{(e/c)^{n+1}N_0{}^{n+1}}\right]^{n/(n+1)}.$$

These two expressions have been coded for computer operation on the raw data.

A final operation is performed to transform the corrected laboratory spectrum to the center-of-mass system,

$$S'(\theta',E')=(E'/E)^{1/2}S(\theta,E).$$

IV. RESULTS AND CONCLUSIONS

21-MeV Bombardment

We have chosen to interpret our data in terms of a simple, semiclassical nuclear model by Ericson and Strutinski.[13] These authors picture the excited compound nucleus as a rotor with moment of inertia $\mathcal{I}$. The rotational energy, therefore, is given by $\frac{1}{2}\mathcal{I}\omega^2=\hbar^2J^2/2\mathcal{I}$ in terms of the nuclear angular momentum J. Consequently, of the total nuclear excitation energy U, only the part $U-\hbar^2J^2/2\mathcal{I}$ is available for intrinsic excitations. If $\rho(U)$ is the level density of a nonrotating nucleus of excitation energy U, this model states that the level density of a system with excitation energy U and angular momentum J is given by

$$\rho(U-\hbar^2J^2/2\mathcal{I})\propto\rho(U)\exp(-\hbar^2J^2/2\mathcal{I}T),$$

where T is the nuclear temperature.

A derivation of the spin dependence of the level density may also be made by considering a random coupling of the angular momenta of ν excited particles. Comparison of the resulting expression with that above yields the relations

$$\sigma^2=\nu\langle m^2\rangle=\mathcal{I}T/\hbar^2, \quad (1)$$

where $\langle m^2\rangle$ is the mean square of the projection of the individual spins on some arbitrary axis. For excitation energies high enough so that the nuclear temperature is not much different from the thermodynamic temperature the relation

$$\mathcal{I}=\hbar^2g_0\langle m^2\rangle \quad (1a)$$

is valid where g_0 is the single-fermion level density at the top of the Fermi sea.

The compound-nucleus problem is solved considering the restrictions imposed by conservation of angular momentum. The differential cross section for the emission of a particle ν with energy E_ν in the direction $\mathbf{n}$ is given by

$$\sigma(\mathbf{n},E_\nu)=\pi\lambda_i{}^2\frac{g_\nu\rho_\nu(U_\nu,0)}{h}\int_0^\infty dI\frac{2IT_I{}^{(i)}}{\rho_c(I)P(I)}\times\int_0^\infty dl\,2lT_l{}^{(\nu)}(E_\nu)e^{-(I^2+l^2)/2\sigma_\nu{}^2}\times\sum_k(-1)^k\frac{(4k+1)}{4\pi}\left[\frac{(2k)!}{(2^kk!)^2}\right]^2\times j_{2k}(iIl/\sigma_\nu{}^2)P_{2k}(\cos\theta), \quad (2)$$

where $T_I{}^{(i)}$ is the transmission coefficient for the formation of a compound nucleus of angular momentum I by an incident α particle, $T_l{}^{(\nu)}(E_\nu)$ is the transmission coefficient for an α particle emitted with angular momentum l and energy E_ν, $\rho_c(I)$ is the density of compound states with spin I, and g_ν is the statistical weight factor of the emitted particle due to its spin.

The more complete expression of Ericson has been written in this way to clarify an approximation we have made in calculating angular distributions. We have assumed that $P(I)$, the total probability per unit time for the decay of a compound system of angular momentum I, is independent of I. It is expected that, when neutron emission predominates, this assumption is reasonable. In any event, this approximation results in the appearance of the compound-nucleus level density in expression (2). In the complete expression this term cancels out because the compound-nucleus level density appears in all level widths.[1,13]

The transmission coefficients T_I and T_l for α particles in the entrance and exit channels were obtained from optical-model calculations. Optical-model parameters[39–42] have been derived from data in the vicinity of 40 and 20 MeV for a limited number of nuclei and these parameters served to restrict the range of our choices. At low energies, the range from 6 to 15 MeV, there is no experimental information to guide our selection of parameters so the same values found effective at higher energies were used.

We have taken for the form of the potential

$$(V+iW)f(r),$$

where the radial dependence is that given by Woods and Saxon[43]

$$f(r)=[1+\exp(r-R/a)]^{-1};\quad V=-30\text{ MeV};$$
$$W=-10\text{ MeV};\quad R=1.35A^{1/3}+1.30\text{ F};\quad a=0.5\text{ F}.$$

[39] G. Igo, H. E. Wegner, and R. M. Eisberg, Phys. Rev. **101**, 1508 (1956).
[40] G. Igo and R. M. Thaler, Phys. Rev. **106**, 126 (1957).
[41] G. Igo, Phys. Rev. **115**, 1665 (1959).
[42] R. M. Eisberg and C. E. Porter, Rev. Mod. Phys. **33**, 190 (1961).
[43] R. D. Woods and D. S. Saxon, Phys. Rev. **95**, 577 (1954).

The transmission coefficients thus generated were inserted into expression (2) to calculate angular distributions corresponding to several choices of the spin cutoff parameter σ^2. Because of our assumption that $P(I)=$constant, both the spin cutoff parameter of the compound nucleus σ_i^2, and of the residual nucleus σ_f^2, appear in our expression. To establish a relation between them, we note the approximate proportionality

$$\sigma^2 \propto \mathcal{I}T \propto MR^2T \propto A^{5/3}U^{1/2},$$

where A is the nuclear mass number, so that

$$\sigma_i^2/\sigma_f^2=[(A+4)/A]^{5/3}(U_i/U_f)^{1/2}, \tag{3}$$

where U_i is the excitation energy of the compound nucleus and U_f is that of the residual nucleus. Note that we have ignored any variation of the moment of inertia with excitation energy.

With this relation as a constraint, angular distributions were calculated for several values of σ_i^2 at each of several exit channel energies and compared with the experimental observations. The results of these comparisons for the 21-MeV data appear in Figs. 3(a) through 3(f), where the solid curves are calculated using the values of the spin cutoff parameter noted. We consider ourselves fortunate that in each case the value of σ_i^2 came out the same. The initial compound system, target nucleus plus α particle is the same, regardless of the decay mode, so if this had not happened, we would have had to seek some remedy.

Figure 4 is a plot of the values of σ_f^2 obtained at the several residual nucleus excitation energies, versus the temperature $T=U/[(aU)^{1/2}-2]$ of the residual nucleus. From expression (1) we expect this procedure to yield a straight line whose slope is a measure of the moment of inertia (assuming a weak dependence of the moment of inertia on the excitation energy). The straight line obtained (in the region of the observations) gives

$$\mathcal{I}/\mathcal{I}_R=1,$$

where $\mathcal{I}_R$, the rigid-body moment of inertia, has been calculated taking $r=1.2/A^{1/3}$ F for the nuclear radius.

The second set of points in Fig. 4 was obtained in the following way: Subsequent experimental work[44] on the elastic scattering of 21-MeV α particles from Fe^{58} showed that the optical-model fit at the backward angles could be markedly improved by adopting a new set of parameters which differs from that suggested by Huizenga and Igo[45] only in that the real potential is taken to be 40 rather than 50 MeV

$$V=-40 \text{ MeV}; \quad W=-10.26 \text{ MeV};$$
$$a=b=0.58 \text{ F}; \quad R=1.17A^{1/3}+1.77 \text{ F}.$$

The second set of parameters leads to new values for the transmission coefficients and, subsequently, to new values of the cutoff parameter σ^2 which differ by less than 10% from the original ones. The slope of the curve, however, and the magnitude of the moment of inertia derived therefrom, are hardly affected.

The angular distributions displayed by the 21-MeV data behave as expected in that the lowest energy portions of the evaporation spectrum display the least anisotropy. This is because low-energy α particles carry away little angular momentum so only a few l values contribute to the expression for the angular distribution. At small angles there is a significant departure from symmetry about 90 deg which becomes more prominent as the exit channel energy increases. This is the behavior expected from a direct-interaction contribution to the spectrum.

A temperature measurement can be made in the customary way, if we assume the constant temperature form for the level density. The energy distribution of evaporation products is[46,47]

$$n(E) \propto E\sigma_c(E)e^{E/T_c}, \tag{4}$$

where σ_c is the inverse cross section for formation of a compound nucleus and T_c is the nuclear temperature.

The question, as always, is what to use for $\sigma_c(E)$. It is customary to calculate transmission coefficients from an optical model and use

$$\sigma_c=\pi\lambda^2\sum_l(2l+1)T_l. \tag{5}$$

Aside from the objection that this calculation refers to the cross section of a nucleus in its ground state, this procedure is not quite legitimate since it is inconsistent with expression (2) which we are using as the basis for interpreting our results. We have found that the more correct calculation incorporating the spin-dependent level density, yields an insignificant difference in the shape of the emitted particle spectrum. Therefore, our present calculation is the customary one based on Eq. (5) and derived from optical-model methods. The results of these calculations appear in Fig. 5. For our present purpose of calculating a temperature, the shape of σ_c versus E_α is the important thing. We find reasonably good agreement with the results of calculations by others.[34]

Plotting $\ln[n(E)/E\sigma_c]$ versus E yields a reasonably straight line whose slope is a measure of the temperature. This appears in Fig. 6.

The fact that the angular distribution is a function of excitation energy suggests that the slope of the $\ln[n(E)/E\sigma_c]$-versus-E curve will depend on the angle at which it is measured. In particular we expect that the temperature measured in this way will be smallest at 90 deg. A test of this effect was made. However, the variation found, although in the right direction, was of the same size as the uncertainty (7%) in the tem-

[44] J. Benveniste, C. B. Fulmer, and A. C. Mitchell (unpublished).
[45] J. R. Huizenga and G. Igo, Nucl. Phys. **29**, 462 (1962).
[46] L. E. H. Trainer and W. R. Dixon, Can. J. Phys. **34**, 229 (1956).
[47] T. Ericson, Nucl. Phys. **11**, 481 (1959).

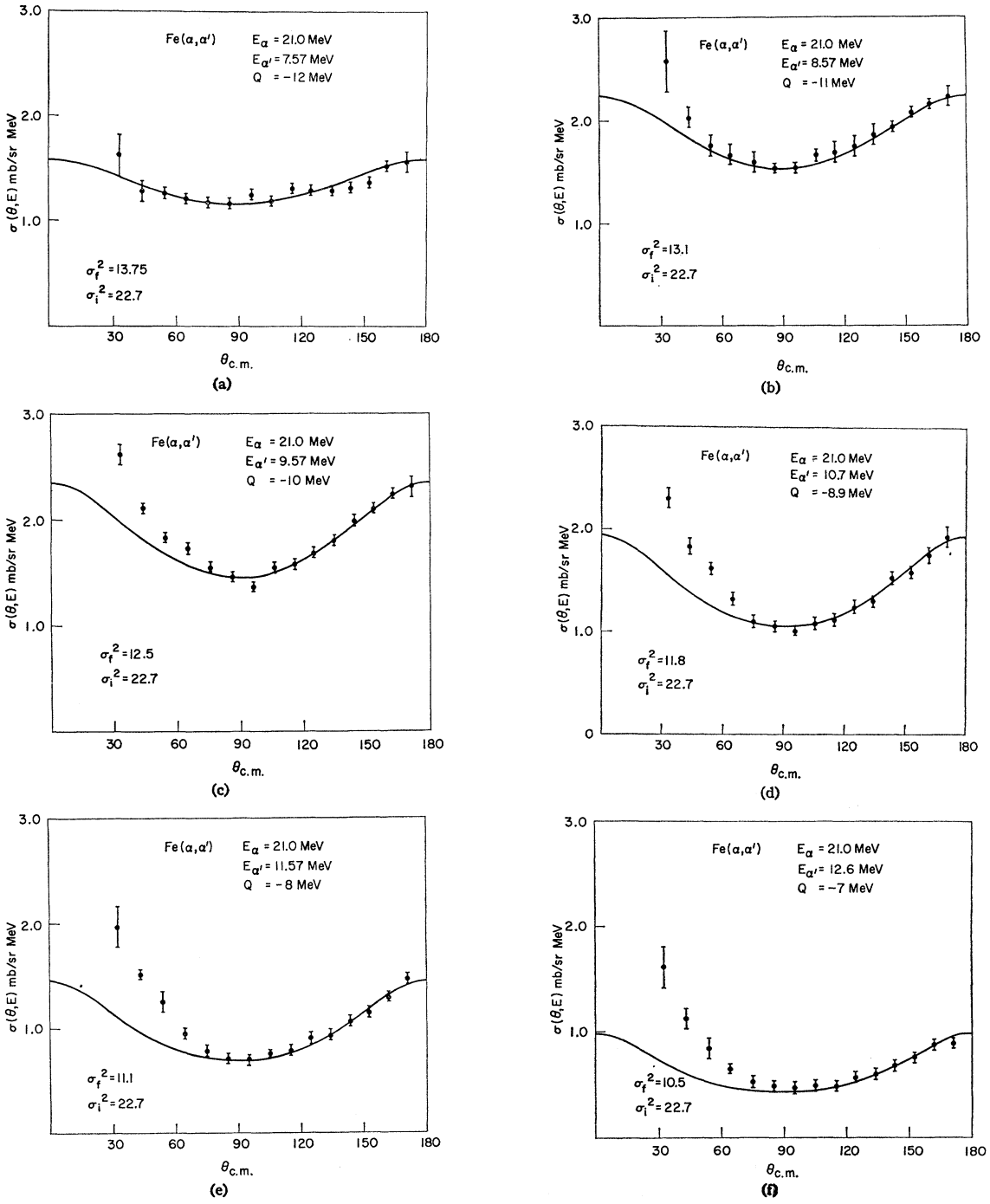

FIG. 3. (a) Angular distribution data for 21-MeV incident α particles, $E_{\alpha'}=7.57$ MeV; (b) angular distribution data for 21-MeV incident α particles, $E_{\alpha'}=8.57$ MeV; (c) angular distribution data for 21-MeV incident α particles, $E_{\alpha'}=9.57$ MeV; (d) angular distribution data for 21-MeV incident α particles, $E_{\alpha'}=10.7$ MeV; (e) angular distribution data for 21-MeV incident α particles, $E_{\alpha'}=11.57$ MeV; (f) angular distribution data for 21-MeV incident α particles, $E_{\alpha'}=12.6$ MeV.

perature measurement. The number reported, $T=1.4$ MeV, is the average of the values found at several back angles.

If, instead, we consider the level-density expression characteristic of a gas of free Fermi particles, then the distribution of evaporated α particles is given by[48]

$$n(E)\propto\frac{E\sigma_c}{(U-\delta)^2}\exp\{2[a(U-\delta)]^{1/2}\},\qquad(6)$$

[48] D. Bodansky, Ann. Rev. Nucl. Sci. **12**, 1962.

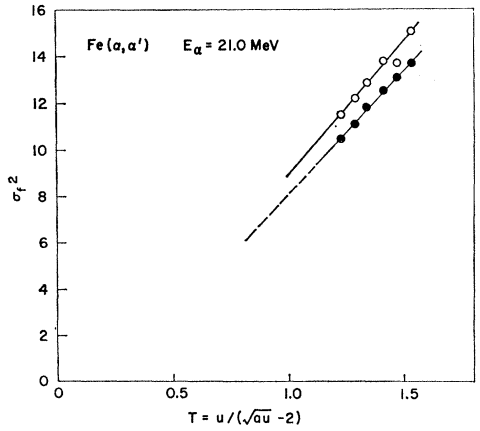

FIG. 4. Plot of values of spin cutoff parameter versus temperature of residual nucleus. The open circles are based on the second set of optical-model parameters described in the text.

where U is the excitation energy of the residual nucleus. Thus, the slope of the curve $\ln[(U-\delta)^2 n(E)/E\sigma_c]$ versus $(U-\delta)^{1/2}$ yields a measure of the constant a. Such a curve appears in Fig. 7. The quantity δ, associated with the excitation energy U, represents the correction for pairing forces after Cameron.[23] The average value of a found from such constructions at several back angles is $a=7$ MeV^{-1}. This is in good agreement with the values reported by other investigators working with other reactions.[49,50]

V. CASCADE-PARTICLE EMISSIONS FROM THE COMPOUND NUCLEUS

The foregoing treatment of the 21-MeV data was simplified by the fact that the energetics of the system will not allow the emission of another nucleon in cascade with the observed α particle in the region of interest. At bombarding energies of 27.5 and 47.9 MeV, however, the energy in the entrance channel is sufficient to permit these cascades. This complexity must be treated in any attempt to understand the observations.

A. Conventional Compound-Nucleus Calculations

For preliminary orientation in the analysis of the 27.5- and 47.9-MeV data we use the conventional compound-nucleus theory, based on the assumption that $\rho(J) \propto (2J+1)$, to estimate the relative importance of multiple-particle emissions to the cross-section measurements described in this paper. We use, in a straightforward manner, the following expression[5]:

$$P_i(U^*,E)dE=\gamma_i\sigma_c E(\rho(U)/\rho(U^*))dE, \qquad (7)$$

where $P_i(U^*,E)dE$ represents the rate at which nuclei excited to U^* will emit the particle i with channel energy between E and $E+dE$; $\gamma_i=g_i m_i/\pi^2\hbar^3$, where g_i is the number of spin states of particle i, and m_i is the reduced mass of particle i. σ_c is the inverse cross section

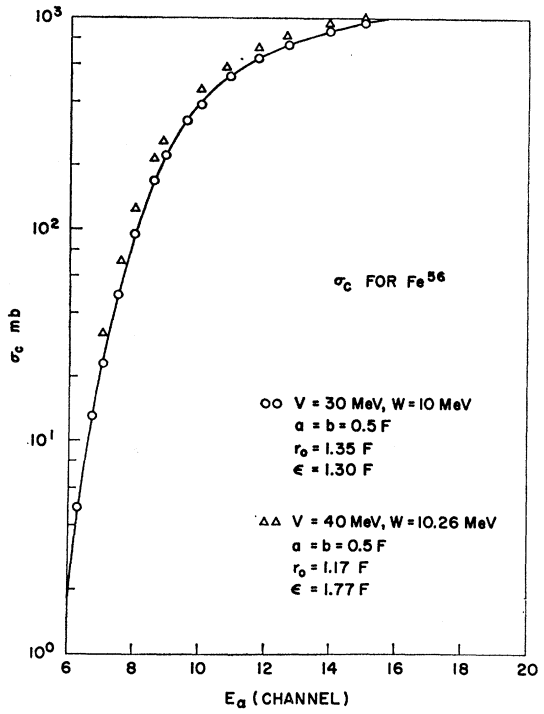

FIG. 5. Optical-model calculations for σ_c, the cross section for formation of a compound nucleus.

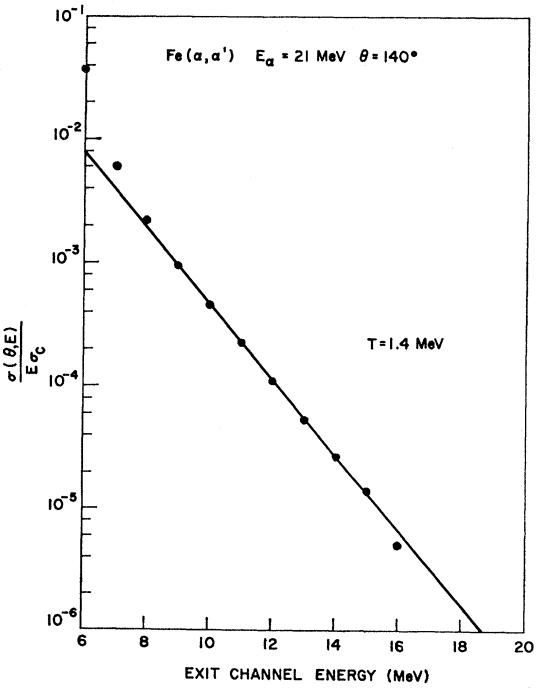

FIG. 6. Nuclear-temperature measurement assuming a constant-temperature level-density expression.

[49] R. Sherr and F. P. Brady, Phys. Rev. 124, 1928 (1961).
[50] U Facchini, *Direct Interactions and Nuclear Reaction Mechanisms* (Gordon and Breach Science Publishers, Inc., New York, 1963), p. 245.

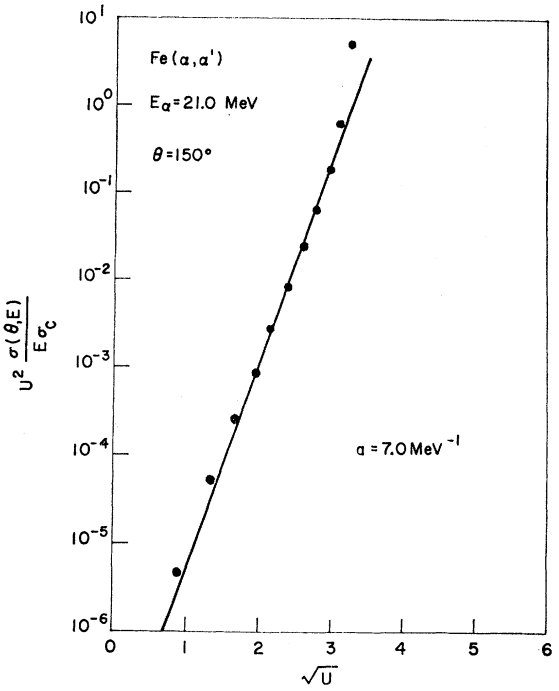

FIG. 7. Measure of a, the level-density constant for a Fermi-gas model of the nucleus.

calculated by means of an optical model of the nucleus. The expression $\rho(U)/\rho(U^*)$ is the ratio of the nuclear energy level density of the residual nucleus at excitation U to the energy level density of the initial nucleus at excitation U^*. The level densities of nuclei excited to energy U are assumed to be given by

$$\rho(U)=C(U-\delta)^{-2}\exp\{2[a(U-\delta)]^{1/2}\}. \quad (8)$$

The value of the parameter a is determined from the 21-MeV data as discussed in Sec. IV. The value of the parameter C is assumed to be constant, and the even-odd parameter δ is 2.8, 1.4, or 0 depending on whether the nucleus is even-even, even-odd, or odd-odd.[23,51]

The numerous permutations and combinations of Eq. (7) corresponding to the various residual nuclei and residual nucleus excitation energies for cascade emissions of n, p, and α particles are calculated to yield the absolute cross sections for $Fe^{56}(\alpha,\alpha')$, $Fe^{56}(\alpha,n\alpha)$, $Fe^{56}(\alpha,p\alpha)$, $Fe^{56}(\alpha,np\alpha)$, and $Fe^{56}(\alpha,2\alpha)$ reactions. Cross sections calculated for incident α particles with energies of 21, 27.5, and 47.9 MeV are shown in Figs. 8 through 10. These calculations indicate that the $Fe(\alpha,\alpha')$ is the only important contributor to the 21-MeV data. The 27.5-MeV data consist primarily of the (α,α') and $(\alpha,n\alpha)$ reactions, while the 47.9-MeV data consist of important contributions from α particles produced by the (α,α'), $(\alpha,n\alpha)$, $(\alpha,2n\alpha)$, $(\alpha,np\alpha)$, and $(\alpha,2\alpha)$ reactions.

When a specific compound nucleus is considered, the maximum of the calculated energy distributions of the emitted α particles shift toward higher emission energies as the excitation energy of the compound nucleus increases. However, cascade emissions from compound nuclei with lower excitation energies prevent the energy distributions of the sum of all α-particle emissions from shifting appreciably to higher emission energies as the bombarding α-particle energy increases. This behavior of the calculated total α-particle emission distributions agrees with the general behavior of the maxima of the experimental energy distributions. Compare Fig. 11 to Fig. 12. Note that the calculated compound-nucleus cross sections have maxima ranging from 9.7 to 10 MeV whereas the experimental distributions have maxima at 9 MeV. It is probably too much to expect more from a conventional calculation.

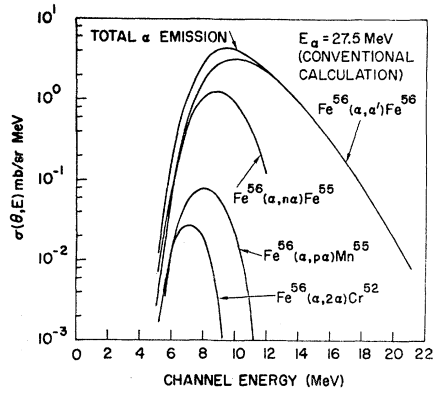

FIG. 9. Cross-section calculations (conventional) for the emission of α particles from the $\alpha+Fe^{56}$ reaction taking into account cascade effects. $E_\alpha=27.5$ MeV.

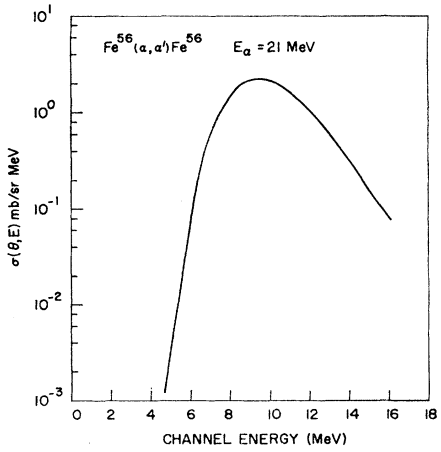

FIG. 8. Cross-section calculations (conventional) for the emission of α particles from the $\alpha+Fe^{56}$ reaction. $E_\alpha=21$ MeV. Cascades turn out to be unimportant.

[51] H. Hurwitz and H. Bethe, Phys. Rev. **81**, 898 (1951).

B. Angular Distributions Involving Multiple-Particle Emission—27.5- and 47.9-MeV Bombardments

The calculations of the preceding section indicate that the interpretation of 27.5- and 47.9-MeV data is complicated by the emission of particles in cascade. A rigorous calculation which considers multiple-particle emissions together with the correct spin dependence of the nuclear level density is unwieldy. Therefore, in the following we estimate the differential cross sections for multiple emissions by assuming that the first nucleon emission [or the first α-particle emission in $(\alpha,2\alpha)$ reactions] is governed by the conventional compound-nucleus theory, and the final α-particle emission leaves the residual nuclei with a nuclear level distribution given by

$$\rho(U,J)=\rho(J)C(U-\delta)^{-2}\exp\{2[a(U-\delta)]^{1/2}\}, \quad (9)$$

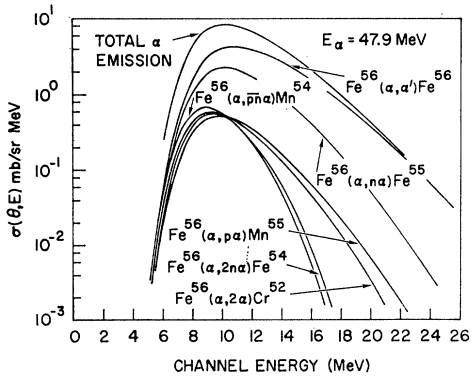

FIG. 10. Cross-section calculations (conventional) for the emission of α particles from the α+Fe^{56} reaction taking into account cascade effects. E_α=47.9 MeV.

where

$$\rho(J)=(2J+1)\exp(-J^2/2\sigma^2).$$

The parameters a and δ are discussed in preceding sections and the value of σ^2, discussed in Sec. IV, is assumed to be given by $\sigma^2=(\sigma_0^2)A^{5/3}T$. For the rigid-rotor model, $\sigma_0^2=\frac{2}{5}MR_0^2\hbar^{-2}$, where M is the nucleon mass and R_0 is the nuclear radius parameter.

Essentially we assume that only the last α-particle emission is accompanied by a significant change in angular momentum and, therefore, only the last α-particle emission yields a residual nucleus with an angular-momentum distribution which differs significantly from that of the original compound nucleus. The simplified treatment may be made plausible with the argument that the emission of one or two neutrons or protons does not remove appreciable angular momentum from the original compound nucleus.

In the calculation of the composite angular distributions, consisting of α particles emitted in cascade as well as those emitted from the original compound nucleus, it is necessary to calculate absolute cross sections for the various combinations of particle emissions so that the cascade emissions can be properly weighted before they are summed. In the following calculations the total decay width $[\Gamma_I=hP(I)]$ appearing in the denominator of Eq. (2) is calculated with the assumption that

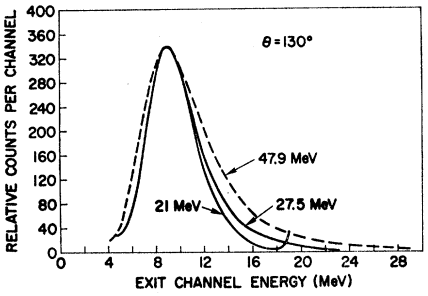

FIG. 11. Experimental energy distributions of α particles emerging from the α+Fe^{56} reaction.

$$\exp\left[-\frac{1}{2\sigma_f^2}(I^2+l^2)+\frac{1}{2\sigma_i^2}I^2\right]j_0(iIl/2\sigma_f^2)\approx 1. \quad (10)$$

Expression (10) is based on the realization that the greatest contributions to Γ_I occur for values of l which are less than 2 or 3.

Equation (2) can be integrated over the scattering angle θ to obtain

$$\sigma(E_\nu)=\frac{\gamma_\nu\rho_\nu(U_\nu^*,0)}{\gamma_c\rho_c(U_c,0)}\pi\lambda_i^2\int_0^\infty dI\,2IT_I^{(i)}\int_0^\infty\frac{dl\,2lT_l^{(\nu)}}{4\pi\Gamma_I}\times\frac{\exp[-(I^2+l^2)/2\sigma_\nu^2]}{\exp[-I^2/2\sigma_i^2]}j_0(iIl/2\sigma_\nu^2). \quad (11)$$

In the calculation of neutron and proton emissions we assume that assumption (10) also holds for the numera-

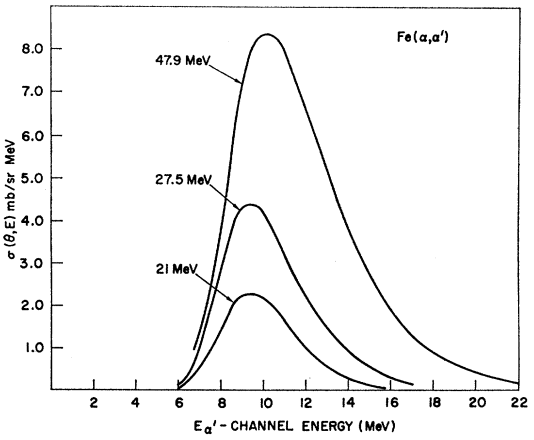

FIG. 12. Calculated energy distributions of α particles emerging from the α+Fe^{56} compound nucleus.

tor of expression (11). With this final approximation our method of data interpretation reduces to an initial conventional compound-nucleus calculation and a subsequent calculation using Eq. (2) to describe the final α-particle emission.

With Eqs. (7) and (8), and the parameters a and δ

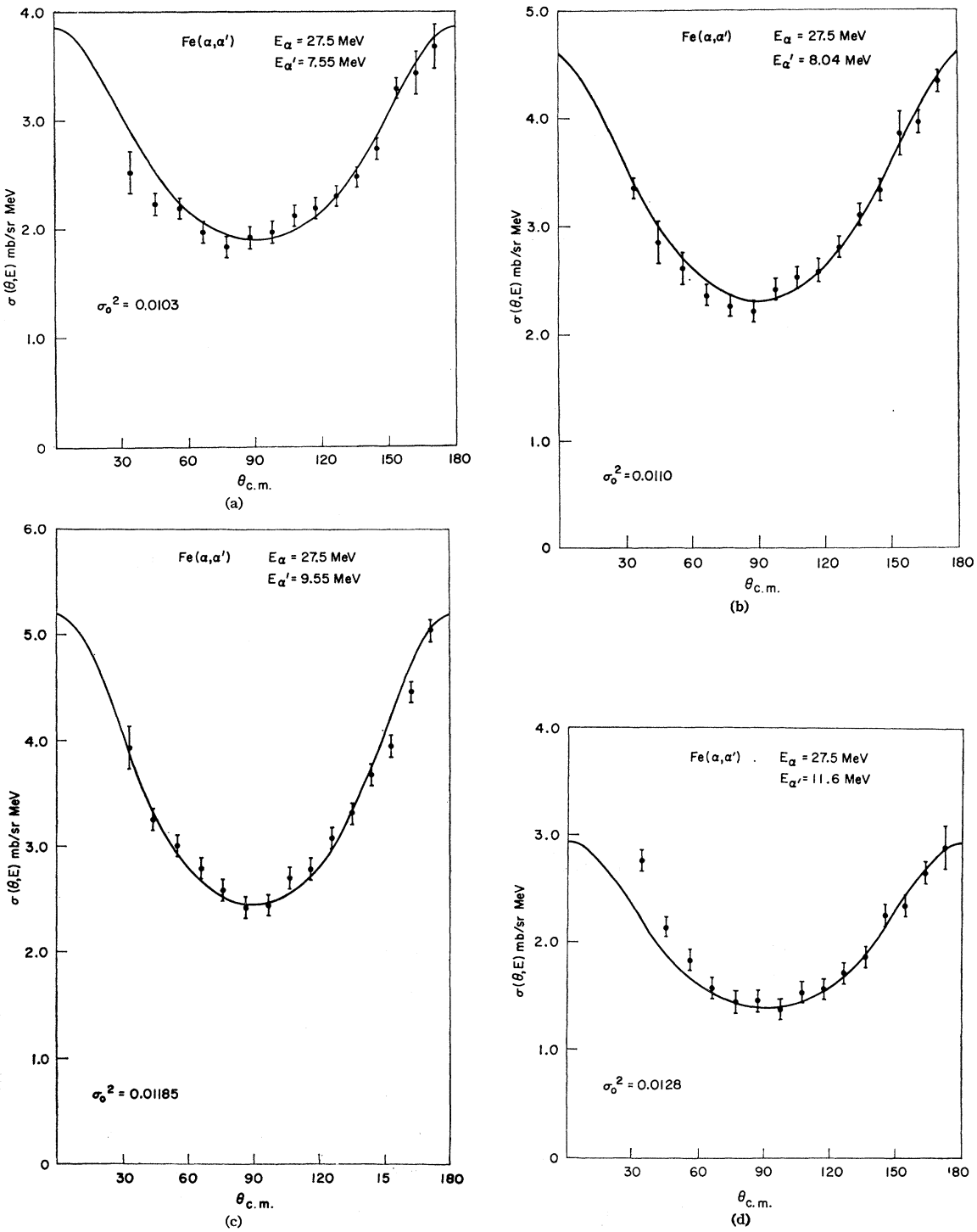

FIG. 13. (a) Angular-distribution data for 27.5-MeV incident α particles, $E_{\alpha'}=7.55$ MeV; (b) angular-distribution data for 27.5-MeV incident α particles, $E_{\alpha'}=8.04$ MeV; (c) angular-distribution data for 27.5-MeV incident α particles, $E_{\alpha'}=9.55$ MeV; (d) angular-distribution data for 27.5-MeV incident α particles, $E_{\alpha'}=11.6$ MeV.

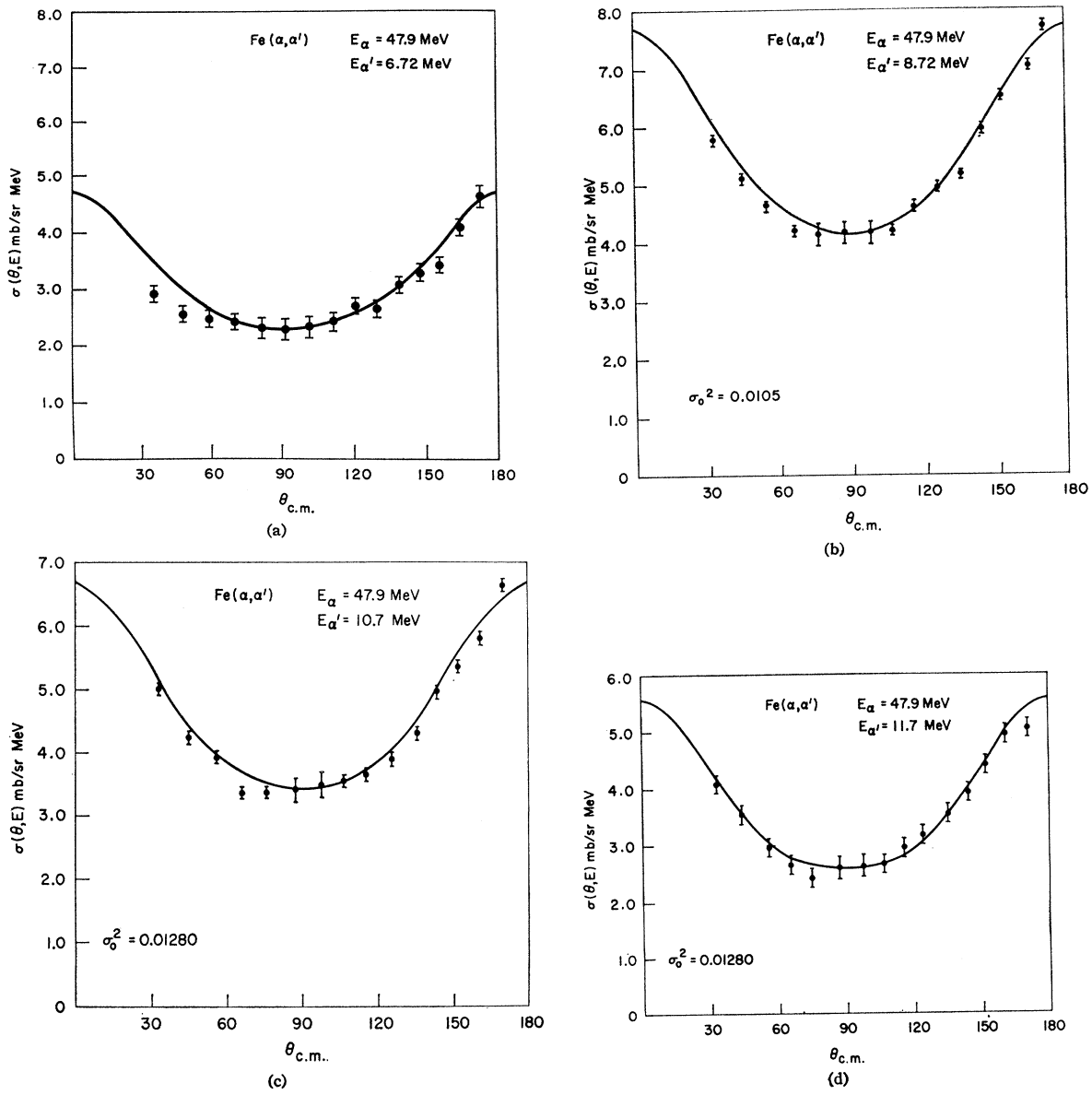

FIG. 14. (a) Angular-distribution data for 47.9-MeV incident α particles, $E_{\alpha'}=6.72$ MeV. This angular distribution is discussed more fully in Sec. VC; (b) angular-distribution data for 47.9-MeV incident α particles, $E_{\alpha'}=8.72$ MeV; (c) angular-distribution data for 47.9-MeV incident α particles, $E_{\alpha'}=10.7$ MeV; (d) angular-distribution data for 47.9-MeV incident α particles, $E_{\alpha'}=11.7$ MeV.

discussed in Sec. IV we calculate the cross sections for the residual nuclei produced by Fe(α,n), Fe$(\alpha,2n)$, Fe(α,p), and Fe(α,α) reactions when Fe is bombarded with 27.5- and 47.9-MeV incident α particles. These residual nucleus excitation energy distributions are the basis for our calculation of the angular distributions for the $(\alpha,n\alpha)$, $(\alpha,p\alpha)$, $(\alpha,2n\alpha)$, $(\alpha,pn\alpha)$, and $(\alpha,\alpha\alpha)$ reactions. Equation (2) is used to calculate the α-particle emission angular distributions from these various residual nuclei. The values of T_I and T_l used in calculating the secondary α-particle angular distributions were obtained from optical-model calculations for α particles incident on Fe^{56}. Figures 13 and 14 show the theoretical angular distributions obtained by summing the various calculated angular distributions, e.g., (α,α'), $(\alpha,n\alpha)$, etc., superimposed on the experimental points. The most appropriate value of σ_0 for making the match is noted on the figures. [The results of the 27.5-MeV theoretical calculations shown in Figs. 13(a) to 13(d) are based on a modified procedure which is fully discussed in Sec. VB.]

In the interpretation of the 21-MeV data we found that, within the limits of our assumptions, $\sigma_f^2=\sigma_0^2A^{5/3}T$ where $T=U/[(aU)^{1/2}-2]$. As can be seen by comparing the 21-MeV values of σ_f^2 in Fig. 5 with the same values

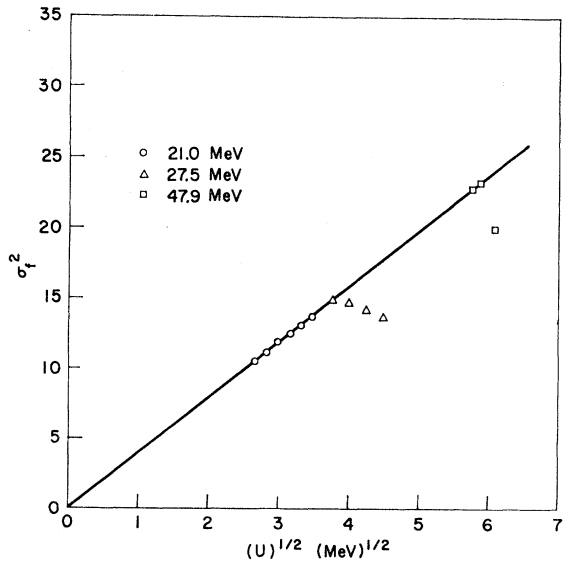

FIG. 15. Summary of σ_f^2 values obtained from 21-, 27.5-, and 47.9-MeV data.

of σ_f^2 in Fig. 15, the nuclear temperature could just as well be assumed to be given by the high-energy asymptotic value[52] $T=(U/a)^{1/2}$. The assumption that $\sigma_f^2 = (2MR_0^2/5\hbar^2)A^{5/3}T$, corresponds to the Fermi gas theory prediction.[11] The only effect of using the different definitions of temperature is a change in the value of the parameter $\sigma_0^2=2MR_0^2/5\hbar^2$ that is deduced from the comparison of calculated and experimental 21-MeV angular distributions.

In the case of the 21-MeV data only one value of the residual nucleus excitation energy U_i and therefore only one value of σ_f^2 is involved for each α-particle angular-distribution energy. For the 27.5- and 47.9-MeV data the inelastically scattered α particles of a specific kinetic energy which are not emitted from the original compound nucleus can correspond to a range of residual nuclei. Nevertheless, according to the rigid-rotor model or Fermi-gas model we should be able to use the same value of the parameter σ_0^2 for all of the various residual nuclei that contribute to a specific angular distribution, this includes the discrete-energy residual nucleus corresponding to α-particle emission from the original compound nucleus. In our analysis, therefore, we assume that all the residual nuclei contributing to a specific angular distribution have the same value of σ_0^2.

The values of σ_0^2 used to obtain calculated angular distributions that match the various α-particle emission energies should, in principle, be equal. The actual values of the parameter σ_0^2 corresponding to the calculated curves that match the 47.9- and 21-MeV experimental angular distributions [we assume that $T=(U/a)^{1/2}$] are given in Table I. These values agree to within 25%. The values of σ_0^2 used in obtaining the calculated curves can be related to a nuclear-radius parameter. These are also given in Table I. (The portion of Table I pertaining to the 27.5-MeV data is based on a somewhat altered treatment involving a number of additional considerations which are discussed in Sec. VD.) In Table II the experimental differential cross sections at 90 deg are compared with the calculated 90-deg differential cross sections. Figure 15 shows the values of σ_f^2 corresponding to the discrete-energy residual nuclei produced by α-particle emission from the original compound nucleus.

[52] If $\rho(U)\propto U^{-n}\exp[2(aU)^{1/2}]$ then $1/T=(a/U)^{1/2}-n/U$.

C. Trapped Alpha Particles

The calculation of the inelastic scattering distribution for the 47.9-, 6.72-MeV case with the procedure described in Sec. VB results in a cross section that is at least an order of magnitude smaller than the experimental cross section. This divergence may be the result of our simplifying assumption that Γ_I is not a function of I, an assumption that is reasonable as long as the principal contributions to Γ_I come from neutron and proton emission. There are so-called trapped α-particle situations, however, in which the emission of low-energy α particles from nuclei with low excitation energies is enhanced because only an α particle can remove the

TABLE I. Values of the parameter σ_0^2 and the corresponding nuclear-radius parameter R_0 that yield calculated angular distributions consistent with the various experimental angular distributions.[a]

E_α (MeV)	$E_{\alpha'}$ (MeV)	σ_0^2 (MeV^{-1})	Nuclear radius parameter corresponding to residual-nucleus moment of inertia R_0 (F)	Type of calculation
47.9	11.7	0.0128	1.37	Multiple-particle emission[b]
47.9	10.7	0.0128	1.37	
47.9	8.72	0.0105	1.23	
47.9	6.72	...	...	
27.5	11.6	0.0128	1.37	Multiple-particle emission (hybrid calculation[c])
27.5	9.55	0.01185	1.32	
27.5	8.04	0.0110	1.27	
27.5	7.55	0.0103	1.23	
21.0	12.6	0.0128	1.37	Single-particle emission[b,d]
21.0	11.57	0.0128	1.37	
21.0	10.7	0.0128	1.37	
21.0	9.57	0.0128	1.37	
21.0	8.57	0.0128	1.37	
21.0	7.57	0.0128	1.37	

[a] In our calculations the spin cutoff parameter is assumed to be given by $\sigma^2=\mathcal{I}_{\rm rig}T/\hbar^2=\sigma_0^2A^{5/3}T$, where A is the nuclear mass number and T the thermodynamic temperature of the nucleus; $\mathcal{I}_{\rm rig}=\frac{2}{5}MR_0^2A^{5/3}$, where R_0 is the nuclear-radius parameter, and M is the nucleon mass; therefore, $\sigma_0^2=\frac{2}{5}(MR_0^2/\hbar^2)$.

[b] In the interpretation of the 47.9- and 21-MeV data the temperature T at excitation energy U is assumed to be given by $T=(U/a)^{1/2}$.

[c] In the interpretation of the 27.5-MeV data the first residual nucleus in the cascade is assumed to have a temperature given by $T=(U/a)^{1/2}$; the second residual nucleus is assumed to have a constant temperature, $T_c=1.4$ MeV.

[d] If the "nuclear temperature," $T=U/[(aU)^{1/2}-2]$, is used, the 21-MeV data are consistent with a nuclear-radius parameter equal to 1.2 F.

large angular momentum required for the transition.[53] The $Fe^{56}(\alpha,2n\alpha)Fe^{54}$ reaction has Ni^{58} as an intermediate residual nucleus. Our conventional compound-nucleus calculation indicates that an appreciable portion of the 6.72-MeV angular distribution is produced by secondary α-particle emissions from Ni^{58}. A meaningful calculation of the 6.72-MeV α-particle emission probability would have to be based on the explicit calculation of Γ_I.[54]

The possibility of a divergence between the 27.5-, 7.55-MeV measured and calculated cross sections, caused by trapped α particles, also may be considered. In the case of the 27.5-MeV bombardment the trapped α particles would be emitted from Ni^{59} produced by the $Fe^{56}(\alpha,n)Ni^{59}$ reaction rather than from Ni^{58} produced by the $Fe^{56}(\alpha,2n)Ni^{58}$ reaction. The minimum excitation energy required to emit a 6.72-MeV α particle from Ni^{58} is 12.1 MeV. At this minimum excitation energy the only available neutron emission channel is the ground state of Ni^{57}. At the minimum excitation energy required to emit a 7.55-MeV α particle from Ni^{59} the available neutron emission channels correspond to the many Ni^{58} states with an excitation energy below 4.6 MeV. The foregoing binding energy considerations indicate that trapped α particles are more probable in the 47.9-, 6.72-MeV angular distribution than in the 27.5-, 7.55-MeV angular distribution.

TABLE II. Experimental and calculated Fe(α,α')Fe* differential cross sections for $\theta_{c.m.}=90$.

Bombarding alpha-particle energy E_α (MeV)	Observed alpha-particle energy E_α* (MeV)	Experimental cross section $\sigma(\theta_{c.m.},E_\alpha')$ mb sr^{-1} MeV^{-1}	Calculated cross section $\sigma(\theta_{c.m.},E_\alpha')$ mb sr^{-1} MeV^{-1} a	b
47.9	11.70	2.61	2.61	
47.9	10.70	3.40	2.86	
47.9	8.72	4.04	1.87	
47.9	6.72	2.35	···	
27.5	11.60	1.40	1.40	
27.5	9.55	2.45	3.35	
27.5	8.04	2.30	2.05	
27.5	7.55	1.90	1.59	
21.0	12.60	0.50	0.185	0.75
21.0	11.57	0.80	0.33	1.21
21.0	10.70	1.20	0.54	1.80
21.0	9.57	1.50	0.77	2.30
21.0	8.57	1.70	0.718	1.90
21.0	7.57	1.20	0.40	1.00

[a] The values in the first calculated cross-section column were obtained with the assumption that the final residual nuclei produced by α-particle emission have a spin distribution given by $\rho_J \propto (2J+1)\exp[-J^2/2\sigma^2]$. All other residual nuclei were assumed to have a spin distribution given by $\rho_J \propto (2J+1)$.

[b] The values in the second calculated cross-section column were obtained with the assumption that all residual nuclei have a spin distribution given by $\rho_J \propto (2J+1)$.

[53] A somewhat similar situation can occur in the case of proton emission: N. O. Lassen and V. A. Sidirov, Nucl. Phys. **19**, 579 (1960).

[54] Another consideration that may enter into the interpretation of the 6.72-MeV angular distribution is the reduction of the Coulomb barrier in the highly excited nucleus: E. Bagge, Ann. Physik **33**, 389 (1938); K. J. LeCouteur, Proc. Phys. Soc. (London) **A63**, 259 (1950); A. M. Lane and K. Parker, Nucl. Phys. **16**, 690 (1960); D. W. Lang, Phys. Rev. **123**, 265 (1961).

TABLE III. Values of the parameter σ_f^2 and the corresponding nuclear-radius parameter R_0 that yield calculated angular distributions that match the various 27.5-MeV experimental angular distributions.[a]

E_α (MeV)	E_α' (MeV)	σ_f^2	σ_0^2 (MeV^{-1})	Nuclear-radius parameter corresponding to residual-nucleus moment of inertia $R_0(F)$
27.5	11.6	13.4	0.0118	1.32
27.5	9.55	11.6	0.0929	1.17
27.5	8.04	10.3	0.0702	1.01
27.5	7.55	9.8	0.0723	1.03

[a] The results summarized in this table are based on a statistical-theory calculation in which the nuclear level density of all residual nuclei is assumed to be given by Eq. (9). The 27.5-MeV hybrid results are included in Tables I and II.

D. Alternative Interpretation of 27.5-MeV Angular Distributions

In the interpretation of the 27.5-MeV data we can use the same procedure as used for the 47.9-MeV data. However, the values of σ_0^2 that yield calculated cross sections that match the experimental cross sections (Table III) are smaller than the values of σ_0^2 obtained from the 21- and 47.9-MeV data.

A possible explanation for the relative lack of success in the interpretation of the 27.5-MeV data as compared to the 21- and 47.9-MeV data may be the $(\alpha,n\alpha)$ contribution to the 27.5-MeV angular distributions. An energy distribution of the residual nuclei produced by the $(\alpha,n\alpha)$ reaction calculated by the conventional method described in Sec. VA is shown in Fig. 16. As can be seen the α particles emitted in the $(\alpha,n\alpha)$ reactions produce residual nuclei with very low excitation energies.

Nuclear level density expressions of the form

$$\rho(U,J)=C(2J+1)\exp(U/T_c)\exp(-J^2/2\sigma_c^2) \quad (12)$$

have been proposed for low excitation energies.[26,47] In this expression the parameter T_c is a constant and $\sigma_c^2=\sigma_0^2A^{5/3}T_c$. In Sec. IV the α-particle energy distributions obtained from the 21-MeV data have been shown to be consistent with a constant temperature form of the nuclear energy level density as well as with Eq. (9).

An alternative interpretation of the 27.5-MeV data employs both Eqs. (9) and (12). The first residual nucleus is assumed to have a nuclear level density given by Eq. (9) and the second residual nucleus, the constant-temperature level density given by Eq. (12). The value of T_c in Eq. (12) is obtained from Fig. 9. The results of hybrid cross-section calculations of the cascade decay of the Ni^{60} compound nucleus are shown in Fig. 17. As can be seen from comparison of Figs. 16 and 18 the

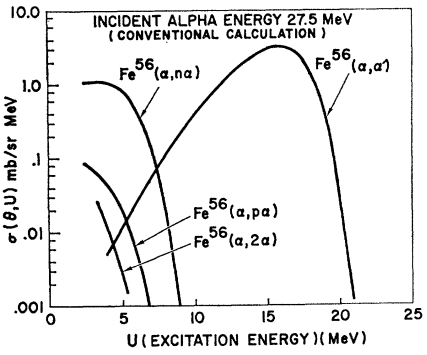

FIG. 16. Excitation energy distribution for residual nuclei resulting from dual-particle emission. $E_\alpha = 27.5$ MeV (conventional calculation).

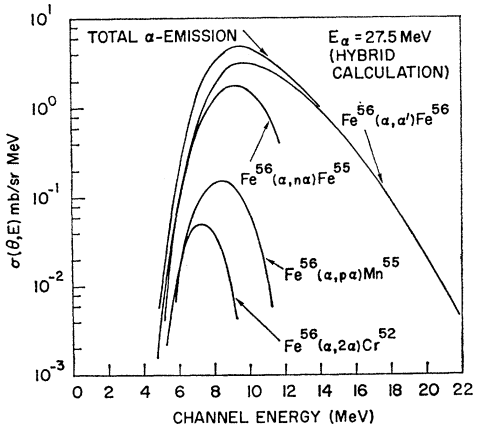

FIG. 17. Cross-section calculations (hybrid) for the emission of α particles from the $\alpha + Fe^{56}$ reaction taking into account cascade effects. $E_\alpha = 27.5$ MeV.

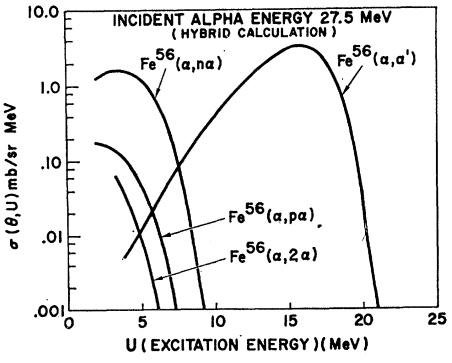

FIG. 18. Excitation energy distribution for residual nuclei resulting from dual-particle emission. $E_\alpha = 27.5$ MeV (hybrid calculation).

probability for the emission of an α particle after the emission of a neutron is increased by assuming a constant temperature level density for the second residual nucleus. As indicated in Table I the hybrid interpretation of the 27.5-MeV data yields values of σ_0^2 and R_0 that are closer to the values obtained from the 47.9- and 21-MeV angular distributions.

VI. SUMMARY

The experimental Fe(α,α')Fe* angular distributions corresponding to α particles emitted with a kinetic energy less than approximately 15 MeV approach symmetry about 90 deg, as predicted by the statistical theory of compound-nucleus reactions. Cross sections corresponding to a relatively large range of residual nucleus excitation energies were measured by bombarding an Fe target with 21-, 27.5-, and 47.9-MeV α particles and observing inelastically scattered α particles with relatively low kinetic energies. The 27.5- and 47.9-MeV bombarding energies were high enough to produce multiple particle emissions, consequently any meaningful compound-nucleus interpretation of the 27.5- and 47.9-MeV data involved the calculation of multiple particle emission cross sections.

An essential purpose of the work described in this paper was to compare the experimental cross sections with compound-nucleus-theory calculations based on nuclear level density expressions derived from specific nuclear models. Ideally, the validity of a specific nuclear model could be tested. We chose to use a simple rigid-rotor model in our statistical-theory calculations. The 21-MeV spectra and angular distributions obtained from Fe gave:

for the nuclear moment of inertia $\mathcal{I}/\mathcal{I}_R = 1$,

for the level density parameter $a = 7\ \text{MeV}^{-1}$,

and for the cutoff parameter $\sigma^2 \cong 12$.

These numbers are consistent with those in the recently reported work of Durham and Halbert.[55] Using these values in the expressions (1) and (1a) derived from the statistical model of the nucleus we find:

for the single-particle level density at the top of the Fermi sea,

$$g = (6/\pi^2)a = 4.2\ \text{MeV}^{-1};$$

for the mean square of the magnetic quantum number,

$$\langle m^2 \rangle = 2$$

which agrees well with Jensen and Luttinger's[56]

$$\langle m^2 \rangle = 0.146A^{2/3} = 2.1;$$

and for the number of nucleons participating in the excitation,

$$\nu = 6.$$

Those parts of the experimental cross sections which are consistent with the compound-nucleus theory are also consistent with a nuclear level density dependency

[55] F. E. Durham and M. L. Halbert, Phys. Rev. **137**, B850 (1965).

[56] J. D. H. Jensen and J. M. Luttinger, Phys. Rev. **86**, 907 (1952).

which, at an excitation of approximately 6 MeV, changes from a Fermi-gas expression of the form given by Eq. (9) to a constant-temperature expression of the form given by Eq. (12). In general, the 21- and 47.9-MeV cross sections are consistent with Eq. (9).

The agreement between the 27.5-MeV experimental data and the statistical-theory calculations is improved when a constant-temperature nuclear level density expression is used for the second residual nucleus in the particle cascade. In the interpretation of cross sections obtained by 27.5-MeV α-particle bombardment, the assumption of a constant nuclear temperature is significant because for this bombarding energy the $(\alpha,n\alpha)$ and $(\alpha,p\alpha)$ decay modes make appreciable contributions to the total α-particle emission probability and result in residual nuclei with $E_{ex}<6$ MeV.

Of the cross-section calculations described in this paper, the magnitude of the 21-MeV experimental and calculated values show the greatest divergence (Table II). The agreement between experimental and calculated cross sections should be improved in a statistical-theory calculation based on explicit evaluation of Γ_I as a function of I.[55,57] A further refinement in the interpretation of the 47.9- and 27.5-MeV cross sections would be the calculation of the changes in the population of spin states in the successive nuclei in particle cascades. Such refinements would involve a significant increase in the expenditure of computer time.

[57] H. F. Bowsher, Bull. Am. Phys. Soc. **9**, 74 (1964); Oak Ridge National Laboratory Report ORNL-TM-971, 1964 (unpublished).

ACKNOWLEDGMENTS

We are indebted to Professor A. C. Helmholtz for permitting the use of the scattering chamber at the 60-in. cyclotron (formerly in Berkeley), to Rex Booth for his invaluable assistance in a number of our cyclotron runs, to Dr. E. Schwarcz for his assistance in calculating optical-model transmission coefficients and compound-nucleus cross sections, to Edna M. Vienop and Mary L. Higuera for their invaluable aid in performing computer calculations, and to Dr. H. M. Blann for the use of his FORTRAN program for the conventional Weisskopf-Ewing statistical-theory calculations. The cooperation of Don Rawles and Dr. W. Barclay Jones and their very competent crews at Livermore and Berkeley, respectively, is greatly appreciated.

Finally, we are grateful to Dr. Torlief Ericson and Professor David Bodansky for several stimulating conversations during the formative stages of this report, and to Dr. J.-P. Hazan for his helpful discussions and critical reading of the manuscript.